Comparison of Multi-microphone Probes and Processing Methods for Acoustic Intensity

Michael Rose

A capstone submitted to the faculty of

Brigham Young University

In partial fulfillment of the requirements for the degree of

Bachelor of Science

Dr. Kent Gee, Advisor

Department of Physics and Astronomy

Brigham Young University

August 2017

Abstract

Comparison of Multi-microphone Probes and Processing Methods for Acoustic Intensity

Michael Rose

Department of Physics and Astronomy

Bachelor of Science

Acoustic intensity measurements traditionally use cross spectral processing methods with multi-microphone probes to estimate pressure and particle velocity. In 2015, Thomas showed that the phase and gradient estimator (PAGE) method increases probe bandwidth without modifying microphone spacing as compared to the traditional cross spectral method. In this study, acoustic intensity is estimated by both the PAGE method and the traditional method across two commercially built 3D intensity probes and three in-house built 2D intensity probes. Probe performance is compared in a broadband, white noise, anechoic sound field radiated from a loudspeaker. Probe orientation is considered by rotating each probe over a 360 degree horizontal plane at 2.5 degree increments. Results show increased frequency bandwidth using the PAGE method across all probe designs. 3D intensity level estimates suffered the least amount of error with the spherical probe. 2D intensity level and direction estimates suffered the least error with the 2D triangular probe with ½" microphones spaced at 2". Measurement limitations concerning the 2D triangular probes with ¼" microphones are discussed

Keywords: Michael Rose, acoustics, multi-microphone probe, phase and amplitude gradient estimator method, PAGE method, vector probe, intensity probe, six-microphone probe, four-microphone probe, p-p technique, scattering, phase mismatch, spatial Nyquist frequency

Acknowledgements

Many thanks go to my wife, Kaia, for staying awake with me during many late nights. She allowed me the time to produce this work and a listening ear whenever I needed it. Thanks to Caleb Goates for also listening to me and answering my many questions. Dr. Traci Neilsen made the writing readability of this work tons better after reading and re-reading this paper as one of the professors of an advanced writing course. Dr. Kent Gee trusted me by offering the opportunity to work on this project. All along the way he taught me about intensity and the PAGE method. Thanks to Dr. Scott Sommerfeldt for his many insights and his availability even with his many responsibilities. Thanks to those who financially supported this work, namely the NSF and the BYU Department of Physics and Astronomy. I see our Father's care through each of you and know that He is and loves me through you.

Table of Contents

List of Figures

Chapter 1: Introduction

Acoustic vector intensity ***I*** has proven useful in many sound engineering and physical applications. It is part of several standardized ways[1,2,3] to obtain radiated power. It is also used in noise source identification,[1,4] for characterizing building insulation,[5,6] and measuring sound emission from noise sources *in situ*.[7] This work's goal is to show a comparison between the traditional intensity estimation method and a new intensity estimation method called the Phase and Amplitude Gradient Estimator (PAGE). In this chapter, section 1.1 gives an overview of intensity, section 1.2 gives a description of three intensity measurement techniques, section 1.3 gives a description of intensity bias errors inherent in each of the three techniques, and section 1.4 gives an outline of the thesis.

1.1 Overview of intensity

Acoustic vector intensity ***I*** is an energy-based quantity. Energy due to a vibration propagates away from the source through a solid or fluid. It is a measure of the rate at which energy is transferred from one element of fluid to an adjacent element per unit area. The transfer of energy has magnitude and direction so ***I*** is a vector quantity.

Intensity $\boldsymbol{I}$ is proportional to sound pressure p and particle velocity $\boldsymbol{u}$. Sound pressure p is the change in pressure in a fluid element relative to the fluid's ambient pressure due to a propagating vibration; u is the velocity imparted to a fluid element from a vibration. Equation 1 shows the frequency domain relationship between $\boldsymbol{I}$, complex pressure p, and $\boldsymbol{u}$; $\boldsymbol{u}^*$ represents the complex conjugate of $\boldsymbol{u}$.

$$\boldsymbol{I}(\omega) = \frac{1}{2}\mathrm{Re}\{p(\omega)\boldsymbol{u}^*(\omega)\} \tag{1}$$

1.2 Intensity measurement techniques

Three techniques for intensity measurement are described: The p-u method, the Traditional method, and the PAGE method.

A direct method for obtaining p and $\boldsymbol{u}$ is the p-u technique. The p-u technique requires an intensity probe[8] called the Microflown that has been developed to measure p and $\boldsymbol{u}$ directly and simultaneously. This method[9] employs two closely spaced heated wires whose resistances are temperature dependent. Particle velocity is obtained from the asymmetric heating of the two wires. In environments where significant non-acoustic temperature and velocity fluctuations occur, the p-u technique has been shown to be less robust than other techniques.[10,11]

In such cases, a more robust technique is the p-p method. This method uses the relationship of the gradient of p, the time derivative of $\boldsymbol{u}$, the medium's ambient density ρ_0, and time t in Euler's equation shown in Equation 2:

$$\rho_0 \frac{\partial \boldsymbol{u}}{\partial t} = -\nabla p. \quad (2)$$

Euler's equation is essentially Newton's second law divided by volume. A pressure gradient for this method is traditionally obtained with an intensity probe that has multiple microphones spaced a distance d apart. One-dimensional gradients are estimated by taking a finite sum and difference of the complex pressure signals from two microphones. Each additional dimension increases the minimum microphones needed by one. This technique is well described in a textbook by Fahy[12] and in other handbooks.[13,14] This method has bandwidth limitations due to spatial aliasing at or above the spatial Nyquist frequency f_N corresponding to $d \geq \frac{\lambda}{2}$, λ being the wavelength of a sound wave of frequency f.

In response to the bandwidth limitations of the p-p method, there is a new pressure-based intensity estimation method called the Phase and Amplitude Gradient Estimator (PAGE). This method has been shown[15] to accurately estimate $\boldsymbol{I}$ up to f_N. It is inspired by expressions developed by Mann *et al.*[16] and Mann and Tichy[17,18] that relate the active intensity $\boldsymbol{I}_a$ to the complex pressure magnitude P and phase gradient $\nabla\phi$. One of the strengths of the PAGE method is its capability to estimate $\boldsymbol{I}$ above f_N through phase unwrapping, which is described in Sec. 2.2. Notwithstanding this strength, the PAGE method has limitations when the coherence between microphone pairs is low.

1.3 Bias errors

Each intensity estimation method has its own unique bias errors. A bias error is any deviation in the intensity estimate from the actual intensity in the field due to the estimation method or probe geometry. However, the p-p technique assumes a linear variation of the non-linearly varying

complex pressure in estimating the gradient, which introduces bias errors. The PAGE method reduces these types of bias errors by using the complex pressure magnitude and phase gradients, which both vary more linearly than the gradient of the complex pressure.

Multi-microphone techniques have inherent bias errors for low frequencies and for high frequencies. For low frequencies, there is phase mismatch between microphones, represented as an angle in the complex plane, corresponding to a spatial distance for every frequency. When the ratio between the phase difference due to wave propagation between microphones and the phase difference due to microphone phase mismatch is about 1, as shown in Figure 1 (similar to figure 3 in Giraud *et al.*[19]), significant bias errors are introduced. Figure 2 shows the low frequency bias errors that occur for various d. For high frequencies, the dimensions of the microphones on an intensity probe can be on the order of a wavelength. These frequencies scatter off of the microphones rather than diffracting around it. The scattered sound corrupts the signal at other microphones. In addition to scattering, spatial aliasing can bias estimates above f_N.

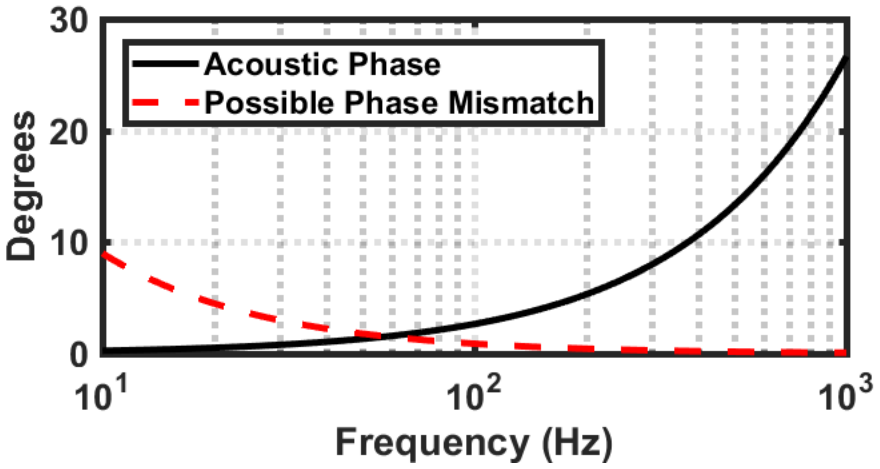

Figure 1: Two ideal microphones spaced a distance $d = 2.54$ cm apart will have an acoustic phase difference due to wave propagation shown as the solid curve. Manufacturing variation yields inherent phase mismatch. One possible phase mismatch is shown as the dashed curve. When the ratio of phase mismatch to acoustic phase difference becomes greater than or equal to 1, significant bias errors occur in $\boldsymbol{I}$.

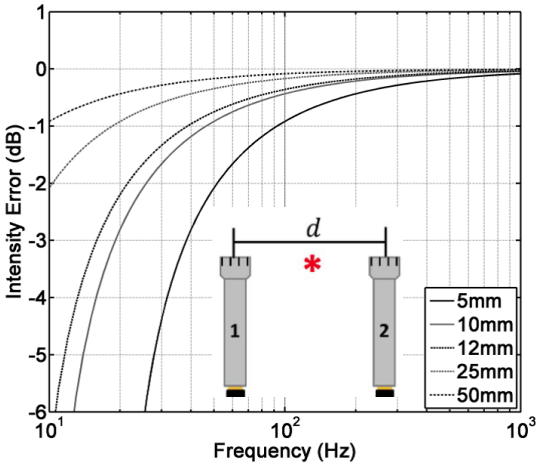

Figure 2: Bias errors in the low frequencies increase as d decreases. When $d = 5$mm, there is a 1 dB error as high as 90 Hz while for when $d = 25$mm, there is a 1 dB error as low as 20 Hz. The larger d is, the lower an intensity estimate can be made accurately.

An understanding of inherent bias errors provides performance expectations based on estimation methods and probe design combinations. For example, a multi-microphone probe

with large inter-microphone spacing is expected to perform well in the low frequencies, while a similar probe with small inter-microphone spacing is expected to provide reliable $\boldsymbol{I}$ in the higher frequencies. A probe with large microphones scatters more at high frequencies than a probe with small microphones. Pressure signals processed with the traditional method are expected to have slightly more bias errors than the PAGE method due to the assumption of a linear complex pressure. The PAGE method is expected to extend the frequency bandwidth.

1.4 Thesis scope and outline

Similar to Weiderhold's work,[20] this work compares pressure-based intensity measurement bias errors for five multi-microphone probes. In addition to comparing multi-microphone probe performance like Weiderhold, I make a comparison of the traditional p-p technique and the PAGE method. Numerical methods are detailed in Chapter 2 for both methods. A description of each intensity probe and the intensity sound field of each probe are in chapter 3. Bias errors for each probe and estimation method combination are presented and discussed in chapter 4.

Chapter 2: Numerical Methods

This chapter presents how acoustic intensity is numerically estimated with the traditional method and the PAGE method in one dimension. Higher dimensional intensity is determined by least-squares formulation of the gradient estimates.

2.1 Traditional numerical methods

The traditional method estimates $\boldsymbol{I}$ by Equation **1** from multiple pressure sensors. Pressure sensors are used to obtain the complex pressure p while particle velocity $\boldsymbol{u}$ is estimated through Equation **2**. These quantities are related by Equation 3. The pressure gradient is defined in the traditional method by

$$\nabla p = \frac{p_2 - p_1}{d}. \tag{3}$$

where $p_1$and p_2 refer to the pressure seen by a pair of microphones and d refers to the distance separating them. Although these formulations are what the traditional method is based on, Fahy[21] and Pavic[22] show that in practice the traditional one-dimensional intensity $\boldsymbol{I}^{\mathrm{TRAD}}$ can be written in terms of the quadspectrum,

$$\boldsymbol{I}_{1\mathrm{D}}^{\mathrm{TRAD}}(\omega) = \frac{1}{\rho_0 \omega d} Q_{12}(\omega), \tag{4}$$

where ω is the angular frequency of the sound wave. Multi-dimensional $\boldsymbol{I}^{\mathrm{TRAD}}$ is obtained by a least squares weighting of quad spectra as described by Pascal and Li.[23] A quadspectrum is given as

$$Q_{12}(\omega) = \mathrm{Im}\{p_1^* p_2\}. \tag{5}$$

The traditional method is susceptible to high frequency bias errors. The quadspectrum shows significant bias[20] errors greater than 1 dB at $kd = \frac{2\pi f}{c} d \geq 1.15$ due to spatial aliasing and the linear approximation of the real and imaginary parts of p, where c is the sound speed and k is the wavenumber $\frac{2\pi}{\lambda}$. For a one inch microphone separation, this begins at approximately 2.5 kHz.

2.2 PAGE numerical methods

The PAGE method uses the phase gradient $\nabla\phi$ and complex pressure magnitude P to estimate acoustic intensity $\boldsymbol{I}$ as described theoretically by Mann *et al.*[16] and Mann and Tichy.[17,18] The complex pressure $\tilde{p}$ at a distance $\boldsymbol{r}$ expressed in polar form is dependent on P and ϕ by $p(\boldsymbol{r}) = P(\boldsymbol{r})e^{-j\phi(\boldsymbol{r})}$. By Euler's equation (Eq. 2), the $\boldsymbol{u}$ is dependent on ∇p by,

$$\boldsymbol{u}(\boldsymbol{r}) = \frac{j}{\rho_0 \omega} \nabla p = \frac{j}{\rho_0 \omega} [\nabla P(\boldsymbol{r}) - jP(\boldsymbol{r})\nabla\phi] e^{-j\phi(\boldsymbol{r})}. \tag{6}$$

From Eq. 2, Eq. 8 results in an expression for the active intensity $\boldsymbol{I}^{\mathrm{PAGE}}$ as

$$\boldsymbol{I}^{\mathrm{TRAD}} = \frac{1}{2\rho_0\omega} P^2 \nabla\phi = \frac{1}{\rho_0\omega} \overline{P^2} \nabla\phi, \tag{7}$$

where $\overline{P^2}$ is the mean-square pressure. In practice, $\overline{P^2}$ is obtained by averaging the squared pressure from a microphone located at the acoustic center of the intensity probe or from a least-squares estimate of the center pressure.[20]

The phase gradient $\nabla\phi$ is calculated based on the geometry of the microphones on an intensity probe. For N microphones on an intensity probe, the location of each microphone relative to the center of the probe is $\boldsymbol{r}_{1,2,\ldots,N}$ as outlined in Thomas *et al.*[15] The location of each microphone relative to every other microphone is written in a matrix $\boldsymbol{R}$ as

$$\boldsymbol{R} = [\boldsymbol{r}_2 - \boldsymbol{r}_1| \ldots |\boldsymbol{r}_N - \boldsymbol{r}_{N-1}]^T. \tag{8}$$

The least-squares estimate for the gradient is expressed as

$$\boldsymbol{\nabla\phi} \approx (\boldsymbol{R}^T\boldsymbol{R})^{-1}\boldsymbol{R}^T\Delta\boldsymbol{\phi}. \tag{9}$$

The ensemble-averaged (or overall) phase difference between microphones $\Delta\boldsymbol{\phi}$ is found through the argument of the transfer function between different microphone pairs, written as

$$H_{12} = \frac{p_1^* p_2}{p_1^* p_1} \tag{10}$$

and

$$\Delta\boldsymbol{\phi} = -[\arg\{H_{12}\}| \ldots |\arg\{H_{(N-1)N}\}]^T. \quad (11)$$

The significant strength of the PAGE method is the capability to estimate $\boldsymbol{I}$ up to $kd = \frac{\pi}{2}$ and then overcome spatial aliasing by unwrapping the 2π phase jump in $\boldsymbol{\Delta\phi}$ above $kd = \frac{\pi}{2}$ for broadband sources. This allows for accurate estimates of $\boldsymbol{I}$ above f_N.

Chapter 3: Experimental Setup

This chapter contains four sections. Section 1 describes each probe being compared. Section 2 describes the experimental setup including: the sound source and type of signal, the geometry of the experiment, the use of the anechoic chamber and turntable, and procedure for obtaining recordings for an intensity probe. Section 3 describes how the reference intensity magnitude is defined that is necessary for calculating intensity magnitude bias errors. Section 4 describes how the reference intensity direction is defined that is necessary for calculating intensity direction bias errors.

3.1 Intensity Probes

Two 3-dimensional intensity probes and three 2-dimensional intensity probes are included in this comparison. Both 3-dimensional probes are commercially built and used G.R.A.S. Sound and Vibration intensity probes. All three 2-dimensional probes are in-house built at BYU. The G.R.A.S. intensity probes are included because they are the probes typically used when measuring sound intensity. The 2-dimensional probes have a regular triangle geometry with a center microphone. This geometry is chosen because it uses the minimum microphones for 2-dimensional intensity plus one in the center to directly measure the center pressure. Their

differences include microphone spacing and microphone size in order to demonstrate the effects of microphone spacing and size.

Probe A

Probe A is the G.R.A.S. 3D Vector Probe Head Type 60LK. Microphones are ¼" CCP Flush-Mounted Microphones Set Type 47LV embedded on the surface of a 30 mm diameter sphere in a regular tetrahedron geometry. Figure 3 is a photo of probe A.

Figure 3: Probe A is a G.R.A.S. 3D Vector Probe Head Type 60LK.

Probe B

Probe B is the G.R.A.S. 50VI-1 Vector intensity probe. It includes three pairs of G.R.A.S. 40AI Sound-intensity microphones that have ½" diameter diaphragms spaced $d = 2.5$ cm from the center of the probe. Figure 4 is a photo of probe B. For future reference, there is a physical spacer in between each microphone and the center of the probe.

Figure 4: Probe B is a G.R.A.S. 50VI-1 Vector intensity probe.

Probe C

Probe C is an in-house built 2-dimensional intensity probe. Three outer microphones are placed 60 degrees apart from each other in a regular triangle formation in addition to a microphone at the probe center. The outer microphones are place one inch from the probe center. These microphones are ¼" G.R.A.S. 40BD prepolarized pressure microphones.

Figure 5: Probe C is an in-house built 2-dimensional intensity probe with ¼" microphones with $d = 1$".

Probe D

Probe D is the same as probe C except the microphones are set two inches from the probe center.

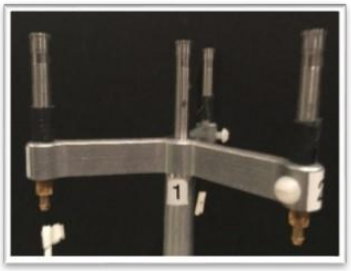

Figure 6: Probe D is an in-house built 2-dimensional intensity probe with ¼” microphones with $d = 2$”.

Probe E

Probe E is the same as probe D except that the microphones are G.R.A.S. 46AE ½” CCP free-field standard microphone sets. These microphones were chosen amongst other similar microphones because they were phase matched.

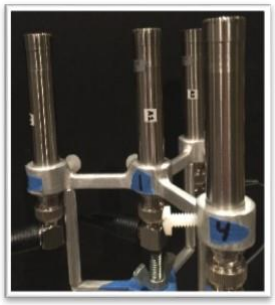

Figure 7: Probe E is an in-house built 2-dimensional intensity probe with ½” microphones with $d = 2$”.

3.2 Experiment Geometry

The sound source and radiated signal type is described here. A Mackie HR624 studio monitor radiated white noise over its entire usable bandwidth of 47 Hz to 20 kHz. Motivation for anechoic chamber choice is seen by the large anechoic chamber provides plenty of room to record far field measurements, it is equipped with turntable, and it removes reflections that would introduce unwanted image sources.

The geometry of the setup includes environment, the location of the loudspeaker and each intensity probe, and the rotation of each probe on a turntable. Figure 8 is a schematic of the setup for easy reference. This experiment is in the large anechoic chamber of Brigham Young University. The loudspeaker is in one corner of the chamber while each intensity probe is on a turntable located in the center of the chamber. Recordings are done by sending a white noise signal through the loudspeaker and recording with an intensity probe for ten seconds. In between each recording, the turntable rotates the intensity probe through 2.5 degrees in a horizontal plane. A full 360 degrees are recorded in this work. Rotating the intensity probes shows how probe orientation affects intensity bias errors due to scattering and pressure gradients.

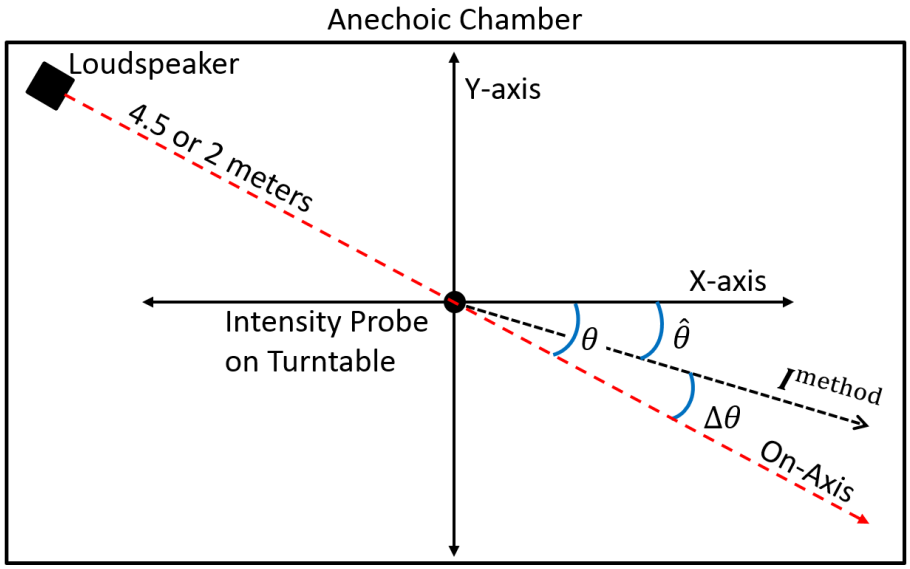

Figure 8: Schematic of the experimental setup. Three angles are shown. First, θ is the angle between the x-axis of the probe and the on-axis direction. Second, $\hat{\theta}$ is the angle between the estimated intensity direction and the probe's x-axis. Third, Δθ is the bias error angle of the estimated intensity direction relative to the known direction.

3.3 Reference intensity magnitude

Intensity magnitude bias errors are calculated based on a reference magnitude measurement. A single microphone can measure sound pressure level (SPL) at a location as shown in Figure 9. When the source to receiver distance is big enough, the sound propagation behaves like a plane wave locally. It is important to note that for a plane wave, SPL and sound intensity level (SIL) are equal. Every probe but probe D is 4.5 meters from the loudspeaker. Using the local plane wave approximation and this property of plane waves, the SPL measured by a single reference microphone is equated to a reference SIL for each intensity probe. An expression for SIL bias error is:

$$L_{\mathrm{I,err}} = 10\log_{10}\left|\frac{\boldsymbol{I}^{\mathrm{METHOD}}}{1\mathrm{pWm^{-2}}}\right| - 20\log_{10}\left|\frac{p_{\mathrm{rms,ref}}}{20\mu\mathrm{Pa}}\right| = L_I^{\mathrm{METHOD}} - L_{p,\mathrm{ref}} \qquad (12)$$

Figure 9: Photo showing a single reference microphone on the turntable with the loudspeaker in the corner of the anechoic chamber.

3.4 Reference intensity direction

Intensity direction bias errors are calculated based on the assumption that sound intensity flows directly away from the loudspeaker at the intensity probe location. Figure 8 shows a schematic that contains three angles important to this discussion. Firstly, as an intensity probe rotates on the turntable, so do the x and y axes. The angle that a probe and the x and y axes rotate through begins from the "On-Axis" direction pointing away from the loudspeaker going clockwise. This is called θ. Another angle $\hat{\theta}$ gives the intensity direction estimated by either the traditional or PAGE method where $\boldsymbol{I} = |\boldsymbol{I}|\left(\cos\left(\hat{\theta}\right)\hat{x} + \sin\left(\hat{\theta}\right)\hat{y}\right)$. This angle is measured from the x axis. Finally, the difference between θ and $\hat{\theta}$ is the intensity direction bias error $\Delta\theta$ written as

$$\Delta\theta = \theta - \hat{\theta}. \tag{13}$$

Chapter 4: Results

This chapter presents the frequency-dependent intensity magnitude and direction bias errors for each probe and estimation method. The frequency limitations of each probe are described using the traditional and PAGE methods for estimating both the intensity magnitude and direction. Conclusions about probe performance are offered.

Frequency-dependent ***I*** estimated from the traditional and PAGE methods as each probe was rotated are displayed in Figures 10-14. Intensity magnitude errors calculated with Eq. 12 are displayed in Figures 10-14a,b and intensity direction bias errors calculated with Eq. 13 are displayed in Figures 10-14c,d. The y-axis on each plot shows θ and the x-axis of every plot shows frequencies. The color corresponds to the bias errors calculated with the corresponding equation. In Figures 10-14a,b intensity magnitude error is in decibels, with white representing $L_{I,\mathrm{err}} = 0$ dB. In Figures 10-14c,d intensity direction error is in degrees, with white representing $\Delta\theta = 0°$.

4.1 Commercial 3-dimensional probes

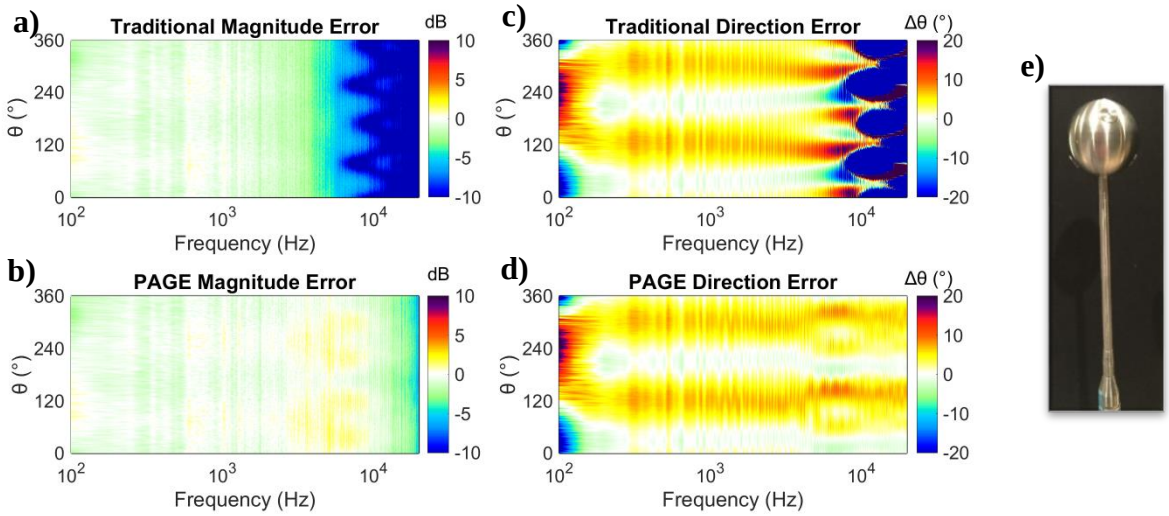

Figure 10: Probe A results. Parts a) and b) show intensity magnitude error in dB and parts c) and d) show intensity direction error in degrees. Parts a) and c) are processed using the Traditional method while parts b) and d) are processed using the PAGE method. Part e) is a photo of probe A.

Probe A, the 3-dimensional spherical probe, has the advantage to estimate 3-dimensional ***I*** but has large scattering effects that affect intensity direction bias errors. The first significant difference is that the traditional intensity estimations have 10 dB error starting around 7.6 kHz as contrasted with the less than 5 dB error using the PAGE method up through the dynamic range of the loudspeaker of up to 20 kHz. A similar trend is seen with the intensity direction error. The traditional estimates vary more than 10 degrees from the reference intensity direction above 8 kHz, while the PAGE method varies less than 10 degrees up through 20 kHz. Two other features are noticeable. First, low frequency $\Delta\theta$ can be explained as low signal to noise ratio combined with phase mismatch errors. Second, $\Delta\theta$ undulates between -5 and +5 degrees depending on θ for both processing methods.

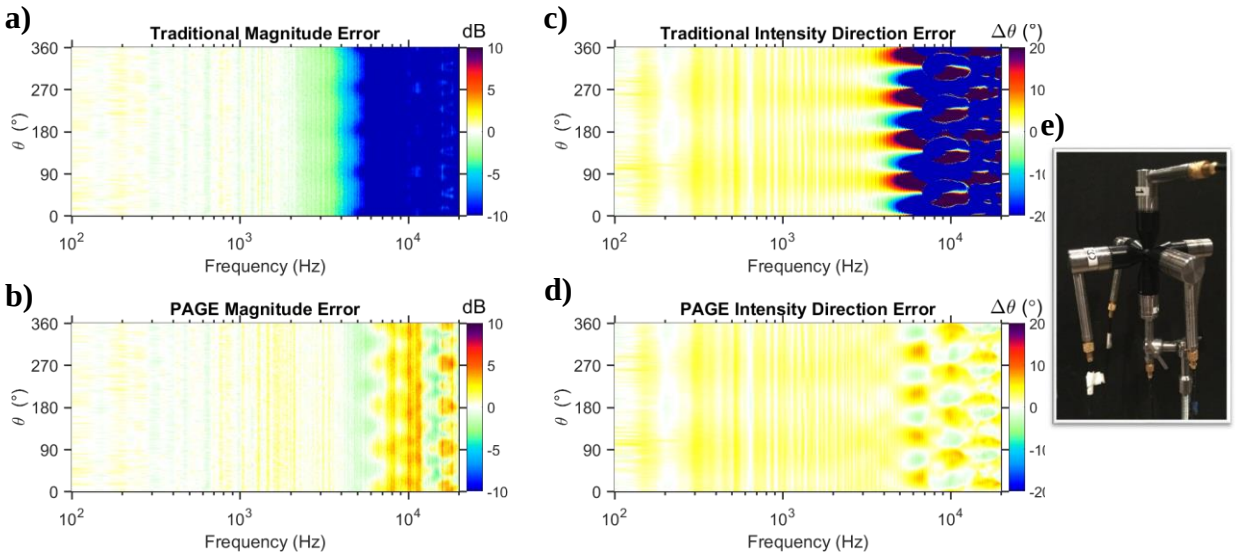

Figure 11: Probe B results. Parts a) and b) show intensity magnitude error in dB and parts c) and d) show intensity direction error in degrees. Parts a) and c) are processed using the Traditional method while parts b) and d) are processed using the PAGE method. Part e) is a photo of probe B.

Probe B, the 3-dimensional orthogonal probe, also has the advantage to estimate 3-dimensional $\boldsymbol{I}$ but has large scattering effects that affect $L_{I,\mathrm{err}}$. Intensity magnitude and direction bias errors estimated by probe B are displayed in Figure 11. Probe B displays similar high frequency intensity magnitude bias errors to probe A, with the distinction that the high frequency limit of probe B is less than that of probe A by 970 Hz. The larger d for probe B than for probe A causes spatial aliasing to occur 1 kHz lower. Larger $L_{I,\mathrm{err}}$ is observed in the 9-20 kHz frequency range using both methods for probe B than for probe A due to scattering caused by the physical spacers. Jacobsen[24] observed that diffraction effects from physical spacers compensate for the finite difference approximation error when microphones are positioned in the face-to-face arrangement. Jacobsen discovered that optimal compensation occurs when microphones are separated by a physical spacer the length of one microphone diameter. Unfortunately, the ½ inch microphones of probe B are separated by spacers nearly two inches long. In addition, the

traditional (finite difference) method is band limited below f_N which does not show the 3-5 dB bias errors above f_N due to scattering shown in Fig. 11b and 11d.

Intensity direction bias errors are less dependent on θ for probe B than for probe A. However, probe B has an overall $\Delta\theta = 5°$ offset that is a discrepancy between the actual probe orientation with respect to the loudspeaker being off by 5° rather than any probe or processing method errors. The PAGE method for probe B shows $\Delta\theta$ values of ±5° due to signal corruption from high frequency scattering beginning at 7 kHz.

4.2 BYU 2-dimensional probes

This section looks at the 2-dimensional 4-microphone intensity probes. Important comparisons are for $L_{I,\mathrm{err}}$ and $\Delta\theta$ depending on microphone spacing and size.

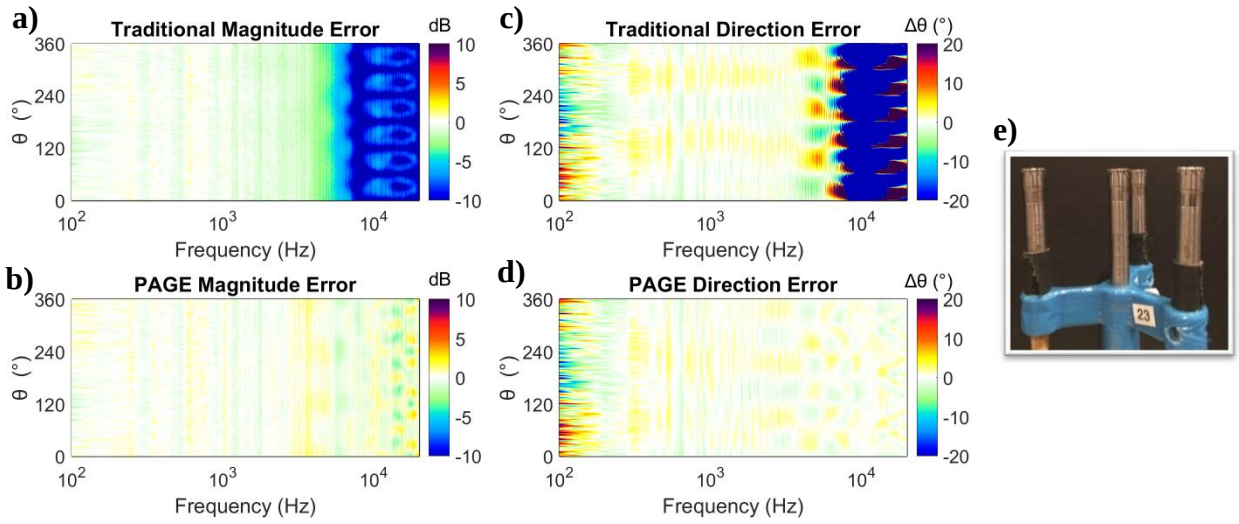

Figure 12: Probe C results. Parts a) and b) show intensity magnitude error in dB and parts c) and d) show intensity direction error in degrees. Parts a) and c) are processed using the traditional method while parts b) and d) are processed using the PAGE method. Part e) is a photo of probe C.

Probe C continues the high frequency limitation trend while using the traditional processing method. The traditional method limits $|\boldsymbol{I}|$ and $\hat{\theta}$ estimates to below 3.9 kHz. However, the PAGE method increases the $|\boldsymbol{I}|$ usable bandwidth because $L_{I,\mathrm{err}} < 5$ dB above f_N. Also, the PAGE method $\Delta\theta$ above f_N is less than ±5°. These ¼" microphones have a high noise floor at low frequencies. Low frequency direction errors for probe C are due to both the low signal to noise ratio and phase mismatch error.

`

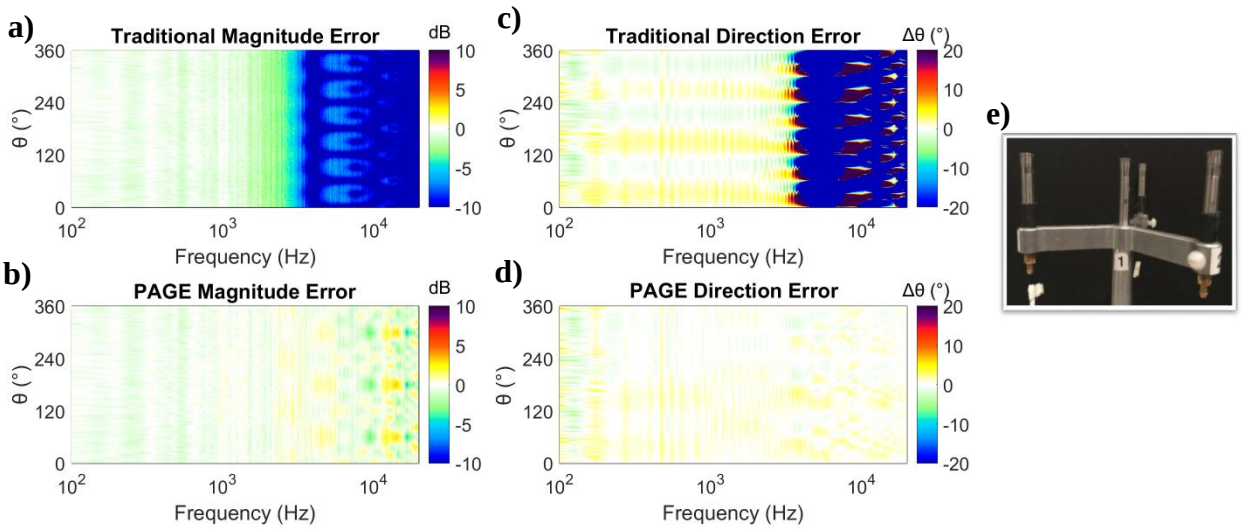

Figure 13: Probe D results. Parts a) and b) show intensity magnitude error in dB and parts c) and d) show intensity direction error in degrees. Parts a) and c) are processed using the Traditional method while parts b) and d) are processed using the PAGE method. Part e) is a photo of probe D.

Once again, traditional method limit estimates of $|\boldsymbol{I}|$ and $\hat{\theta}$ to frequencies below $f_N = 1.9$ kHz. The PAGE method increases the intensity probe's frequency bandwidth beyond f_N all the way to the loudspeaker's frequency limit of 20 kHz. Probe D estimates of $|\boldsymbol{I}|$ and $\hat{\theta}$ with the PAGE method above f_N have $L_{I,\mathrm{err}} < 3$ dB and $\Delta\theta < 3°$. Low frequency $\Delta\theta$ is reduced

compared to probe C because d is increased and the loudspeaker was placed at two meters (as opposed to 4.5 meters) to bring the low frequencies out of the noise floor.

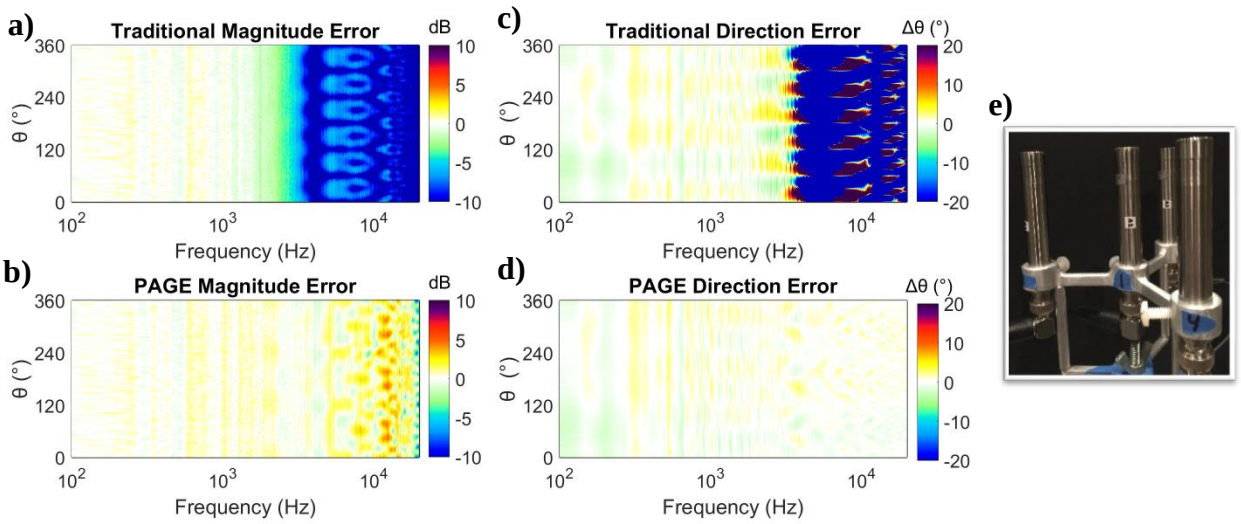

Figure 14: Probe E results. Parts a) and b) show intensity magnitude error in dB and parts c) and d) show intensity direction error in degrees. Parts a) and c) are processed using the Traditional method while parts b) and d) are processed using the PAGE method. Part e) is a photo of probe E.

Probe E completes the pattern that the traditional method limits the probe frequency bandwidth to $f_N = 1.9$ kHz. The PAGE method increases the frequency bandwidth beyond f_N. The ½" microphones on probe E scatter higher frequencies more than quarter-inch microphones on probes C and D; thus $|\boldsymbol{I}|$ estimates for probe E have $L_{I,\mathrm{err}} > 5$ dB beyond f_N. The ½" microphones are well phase matched to 0.1 degrees at 100 Hz which explains the minimal direction error at low frequencies.

4.3 Comparison of probe performance

Since probes A and B are 3D intensity probes, they are compared separately from the 2D probes C, D, and E. Probe A has less $L_{I,\mathrm{err}}$ than probe B because probe B has large physical spacers that cause scattering that corrupts $|\boldsymbol{I}|$ estimates, while probe B has less $\Delta\theta$ than probe A.

As for probes C, D, and E, probe C shows that smaller d leads to greater $\Delta\theta$ due to phase mismatch. Probe E shows that larger microphones have larger $L_{I,\mathrm{err}}$ at high frequencies due to scattering.

The traditional and PAGE methods have significant $|\boldsymbol{I}|$ and $\hat{\theta}$ bandwidth differences. The traditional method consistently is bandwidth limited up to f_N. However, the PAGE method consistently increases the frequency bandwidth of each probe above f_N and in this study, up to the 20 kHz high frequency limit of the sound source. Thus, larger d coupled with estimating intensity with the PAGE method yields the least bias errors.

Several key principles relative to intensity bias errors can be made. Wider microphone separation reduces phase mismatch error. This is shown by the reduced phase mismatch error comparing probe D to probe C. Smaller microphone size and wider microphone separation reduces scattering. This is shown by the reduced high frequency magnitude bias errors of probe E as compared to probe D and C. The PAGE method increases the frequency bandwidth, even beyond the spatial Nyquist frequency with phase unwrapping for probes A-E and does the best for probes that implement minimal scattering techniques (smaller microphones and larger inter-microphone spacing.)

Index

Works Cited

[1] T. Astrup, “Measurement of sound power using the acoustic intensity method — A consultant’s viewpoint”, Appl. Acoust., 50(2), 111–123, (1997).

[2] ISO 9614-2:1996, “Acoustics—Determination of sound power levels of noise sources using sound intensity—Part 2: Measurement by scanning”, International Organization for Standardization, (1996).

[3] ISO 9614-3:2002, “Acoustics—Determination of sound power levels of noise sources using sound intensity—Part 3: Precision method for measurement by scanning”, International Organization for Standardization, (2002).

[4] S. Weyna, “The application of sound intensity technique in research on noise abatement in ships”, Appl. Acoust., 44(4), 341–351, (1995).

[5] ISO 15186-1:2003, “Acoustics—Measurement of sound insulation in buildings and of building elements using sound intensity—Part 1: Laboratory measurements”, International Organization for Standardization, (2003).

[6] ISO 15186-2:2010, “Acoustics—Measurement of sound insulation in buildings and of building elements using sound intensity— Part 2: Field measurements”, International Organization for Standardization, (2003).

[7] ISO 11205:2003, “Acoustics—Noise emitted by machinery and equipment—Engineering method for the determination of emission sound pressure levels in situ at the work station and at other specified positions using sound intensity”, International Organization for Standardization, (2003).

[8] R. Raangs, W. F. Druyvesteyn, and H. E. De Bree, “A low-cost intensity probe,” J. Audio Eng. Soc. 51, 344–357 (2003).

[9] De Bree, Hans-Elias. "The Microflown: An acoustic particle velocity sensor." Acoustics Australia 31.3 (2003): 91-94.

[10] F. Jacobsen, “Sound intensity measurements,” in Handbook of Noise and Vibration Control, edited by M. J. Crocker (Wiley, Hoboken, NJ, 2007), pp. 534–548.

[11] J. H. Giraud, K. L. Gee, and J. E. Ellsworth, “Acoustic temperature measurement in a rocket noise field,” J. Acoust. Soc. Am. 127, EL179–EL184 (2010).

[12] F. Fahy, Sound Intensity (Spon, London, 2002), pp. 1–295.

[13] F. Jacobsen, “Sound intensity,” in Springer Handbook of Acoustics, edited by T. D. Rossing (Springer, New York, 2007), pp. 961–1017.

[14] F. Jacobsen, “Sound intensity measurements,” in Handbook of Noise and Vibration Control, edited by M. J. Crocker (Wiley, Hoboken, NJ, 2007), pp. 534–548.

[15] D. Thomas, B. Christensen, and K. Gee, “Phase and amplitude gradient method for the estimation of acoustic vector quantities,” J. Acoust. Soc. Am. 137, 3366–3376 (2015)

[16] J. A. Mann III, J. Tichy, and A. J. Romano, “Instantaneous and time-averaged energy transfer in acoustic fields,” J. Acoust. Soc. Am. 82, 17–30 (1987).

[17] J. A. Mann III and J. Tichy, “Acoustic intensity analysis: Distinguishing energy propagation and wave-front propagation,” J. Acoust. Soc. Am. 90, 20–25 (1991).

[18] J. A. Mann III and J. Tichy, "Near-field identification of vibration sources, resonant cavities, and diffraction using acoustic intensity measurements," J. Acoust. Soc. Am. 90, 720–729 (1991).

[19] J. H. Giraud, K. L. Gee, S. D. Sommerfeldt, T. Taylor, and J. D. Blotter, "Low-frequency calibration of a multidimensional acoustic intensity probe for application to rocket noise," Proc. Meet. Acoust. Soc. Am., 4aNS9 (2011).

[20] Wiederhold, C. P., Gee, K. L., Blotter, J. D., Sommerfeldt, S. D. and Giraud, J. H. (2014). "Comparison of multimicrophone probe design and processing methods in measuring acoustic intensity," The Journal of the Acoustical Society of America 5, 2797-2807.

[21] F. J. Fahy, "Measurement of acoustic intensity using the cross-spectral density of two microphone signals," J. Acoust. Soc. Am. 62, 1057-1059 (1977).

[22] G. Pavic, "Measurement of sound intensity," J. Sound Vib. 51, 533–545 (1977).

[23] J.-C. Pascal and J.-F. Li, "A systematic method to obtain 3D finite-difference formulations for acoustic intensity and other energy quantities," J. Sound Vib. 310, 1093 – 1111 (2008).

[24] F. Jacobsen, V. Cutanda, and P. M. Juhl, "A numerical and experimental investigation of the performance of sound intensity probes at high frequencies," J. Acoust. Soc. Am. 103, 953–961 (1998).